



Two-dimensional subwavelength meta-nanopillar array for efficient visible light absorption

S. Cao, W. Yu, T. Wang, Z. Xu, C. Wang, Y. Fu, and Y. Liu

Citation: [Applied Physics Letters](#) **102**, 161109 (2013); doi: 10.1063/1.4803046

View online: <http://dx.doi.org/10.1063/1.4803046>

View Table of Contents: <http://scitation.aip.org/content/aip/journal/apl/102/16?ver=pdfcov>

Published by the [AIP Publishing](#)



FREE Multiphysics Simulation e-Magazine

DOWNLOAD TODAY >>

COMSOL

Two-dimensional subwavelength meta-nanopillar array for efficient visible light absorption

S. Cao,^{1,2} W. Yu,^{1,a)} T. Wang,¹ Z. Xu,¹ C. Wang,¹ Y. Fu,³ and Y. Liu⁴

¹State Key Laboratory of Applied Optics, Changchun Institute of Optics, Fine Mechanics and Physics, Chinese Academy of Sciences, 3888 Dongnanhu Road, Changchun, Jilin 130033, People's Republic of China

²Graduate University of Chinese Academy of Sciences, Beijing 100039, China

³School of Physical Electronics, University of Electronic Science and Technology of China, Chengdu 610054, Sichuan Province, People's Republic of China

⁴College of Science, Zhejiang University of Technology, Hangzhou 310023, Zhejiang Province, People's Republic of China

(Received 9 January 2013; accepted 12 April 2013; published online 24 April 2013)

We report the extraordinary light harvesting property of a metamaterial-based subwavelength nanopillar array with a periodic arrangement. It is found that the meta-nanopillar array can absorb light efficiently with an average absorptivity of 0.96 over the whole visible waveband with independent of the incoming light polarization state as well as the wide receiving angle of as large as $\pm 60^\circ$. We attribute the efficient light harvesting property of meta-nanopillar array to the synergistic effect of the slow light mode and localized surface plasmon resonant effect.

© 2013 AIP Publishing LLC [<http://dx.doi.org/10.1063/1.4803046>]

Solar energy is regarded as one of the most plenty yet least harvested sources of renewable energy and much effort has been made to develop highly efficient photovoltaic devices. In the past, lots of attentions have been paid to develop various structures such as nanopillar, nanowire, nanocone, and nanohole arrays, and these structures have displayed unique optical and electric characteristics for energy harvesting.^{1–11} In recent years, more efforts have been shifted to metamaterial-based structure due to its extraordinary electromagnetic properties and the metamaterial is suggested to be an alternative material for absorbers.^{12,13} Cui *et al.* recently reported a one dimensional metamaterial-based sawtooth shape absorber that shows good absorptive property in middle infrared waveband.¹² More recently, we have developed a two-dimensional pyramidal shape metamaterial based absorber, which shows the surprisingly high absorptive property in an extraordinary broad waveband ranging from near infrared to long infrared.¹³ While these two studies mainly focused on infrared waveband, the absorptive effect of visible light waveband was unclear. On the other hand, visible waveband has more than 40% of sun light so that the development of light absorber in visible waveband is of great importance.

In this letter, we come up with a metamaterial based novel solar energy absorber working on the waveband of 400 nm–700 nm, i.e., visible light spectrum. The schematic diagram of this kind of new absorber is shown in Fig. 1(a) which is composed of a periodic array of meta-nanopillars on Au film with a thickness of 100 nm. Because of the existence of this thick Au film, there is nearly no transmittance in the optical regime. The period of the meta-nanopillar array is 200 nm. For a single meta-nanopillar, it has a diameter of 110 nm and consists of alternating Au and Si thin films with thickness of $h_A = 10$ nm and $h_S = 20$ nm as illustrated in

Fig. 1(b). The total number of Au/Si pairs (N) is 32. The filling factor (the ratio of the area of meta-nanopillar to the area of a unit cell) is 0.25.

By employing the rigorous electromagnetic analysis method, i.e., finite-difference and time domain (FDTD) algorithm, the absorption spectrum of the periodic subwavelength meta-nanopillar structure can be calculated and is shown in Fig. 2(a). As is shown in Fig. 2(a), such a metamaterial-based nanopillar absorber can achieve an average absorptivity of 0.96 in the whole visible waveband. Fig. 2(b) shows the normal incident absorption spectra under various filling factors (F) while all other parameters are fixed. As can be seen, when F is smaller than 0.25, the absorptivity drops abruptly in the center wavelength of visible waveband, around 550 nm. While, on the other hand, when F becomes larger than 0.25, its absorptivity drops in the whole visible waveband. Fig. 2(c) shows the effect of the total number of metal/dielectric pairs N on absorptivity. The figure clearly shows that with the increment of N, the average absorptivity becomes larger. In another word, the taller the meta-nanopillar is, the better the absorptivity it can reach, which is consistent with the results reported elsewhere.^{7,11} When N is larger than 32, the average absorptivity has no significant increment anymore. On the other hand, taller meta-nanopillar is more difficult for fabrication. Therefore, we assume the optimum N is 32 here. Fig. 2(d) shows the significant effect of the component of metal/dielectric pair on the absorptivity. First, the thickness of the silicon layer (h_S) is changed and the height of the meta-nanopillar and the thickness of the Au layer (h_A) are fixed to be 960 nm and 10 nm, respectively. Clearly, the optimal thickness of silicon film is 20 nm. When h_S is smaller than 20 nm, the average absorptivity drops significantly. While when h_S becomes larger than 20 nm, the fluctuation of the absorptivity in the whole visible waveband becomes smaller. Second, it is found that when Au layer thickness becomes larger than 10 nm, the absorptivity becomes worse. Finally,

^{a)}Author to whom correspondence should be addressed. Electronic mail: yuwx@ciomp.ac.cn

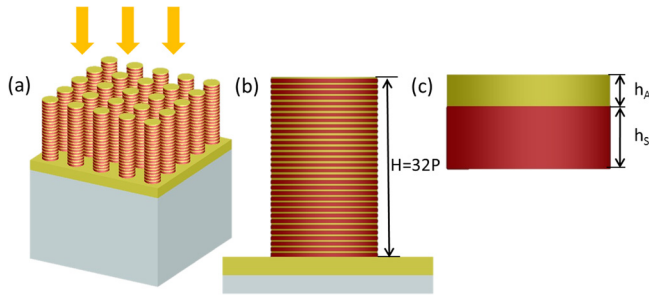


FIG. 1. (a) Schematic diagram of subwavelength periodic meta-nanopillar absorber; (b) cross-sectional view of a single subwavelength meta-nanopillar with Au/Si multilayer stacks; (c) details of one pair of metallic/dielectric thin film stack.

the absorptivity of the pure silicon nanopillar was also calculated and it is found that the average absorptivity of it is far lower than that of meta-nanopillar.

To fully characterize the meta-nanopillar array, the relations between the absorptivity and the wider waveband, the sensitivity of the polarization state as well as the incident angle of incoming light have also been calculated. Fig. 3(a) shows the absorption spectrum of the structure in the waveband of 300 nm–1000 nm. It is shown that though the absorptivity obviously drops down to nearly 0.8 when the wavelength is larger than 800 nm, the average absorptivity in the whole waveband still keeps as high as 0.93. This high absorptivity of meta-nanopillar over the ultra-broad waveband has the incomparable advantage in comparison with the pure Si nanopillar array absorber which only keeps its high absorptivity in the very narrow waveband of 300 nm–400 nm.⁷ Fig. 3(b) shows the absorptivity of the meta-nanopillar absorber under different polarization states of the incident light. As is shown in the figure, the absorptivity of the absorber is almost no change when the polarization angle changes from 0° to 90°. Here, the incident wavelength

is fixed to be 600 nm. This insensitivity of the absorptivity to the polarization state can be attributed to the four-fold rotational symmetry of the meta-nanopillar structure. Figs. 3(c) and 3(d) show the absorption spectra at various incident angles for TM wave and TE wave. As can be seen from the figures, the absorptivity retains up to 0.9 over a wide incident angle of $\pm 60^\circ$ for TM polarization and $\pm 50^\circ$ for TE polarization, respectively. The larger incident angle of TM wave over TE wave is due to the reason that TM polarization has an electric field component along the nanopillar axis and therefore benefits the absorption.⁷

Finally, the physical mechanism of the ultra-broad waveband absorptivity of the meta-nanopillar absorber was analyzed. We investigated the energy flow distribution and y-component of the normalized magnetic field distribution $|H_y|$ in the plane of $y = 0$ at six different wavelengths for the TM polarized wave and the results are shown in Fig. 4 (black arrows depict the Poynting vectors (S)). Unlike the previous reported metamaterial based sawtooth absorber where the slow light modes are considered as the mechanism of light absorbing, here we can only see the obvious similar slow light effect for wavelengths larger than 600 nm where the light propagates into the meta-nanopillar and is trapped inside the nanopillar.¹² However, for wavelengths smaller than 600 nm, it seems that the light is mainly absorbed on the top or edge of the meta-nanopillar, which obviously should not be attributed to slow light effect.

To further find out the absorbing mechanism for wavelengths smaller than 600 nm, the electric field distribution $|E_x|$ for different incident wavelengths was calculated and is shown in Figure 5. From Figure 5, we can clearly observe the electric field hot spots located on the side edge of the meta-nanopillars. These hot spots can obviously be attributed to the localized surface plasmon enhancement effect. This strong local electrical field intensity enhancement can be

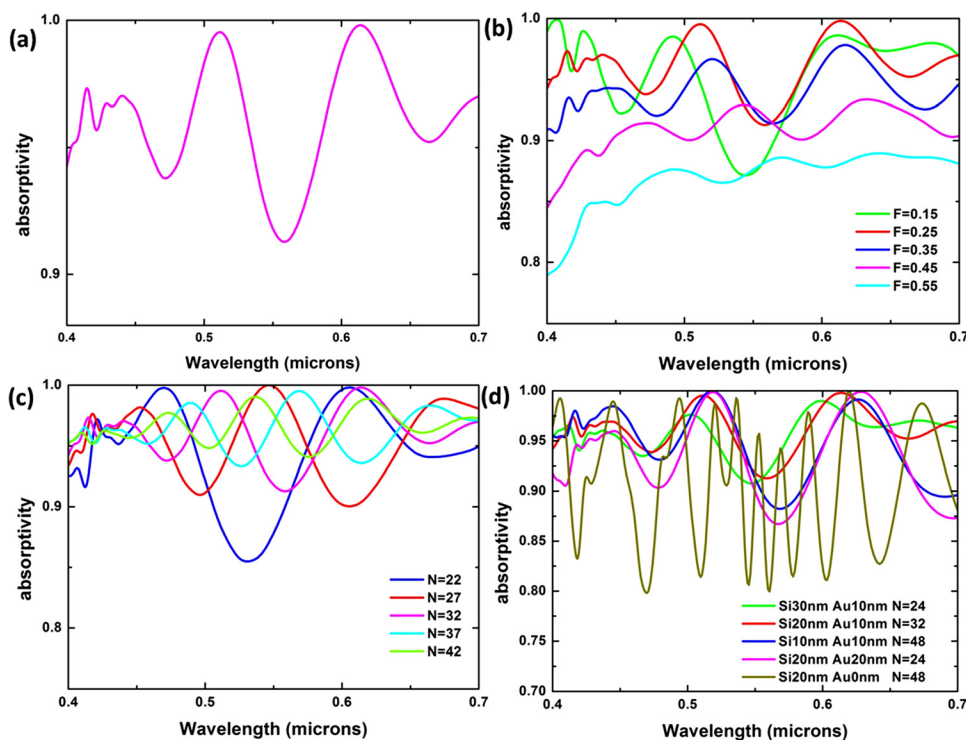


FIG. 2. Absorption spectra of the meta-nanopillar absorber under normal incident light for various conditions. (a) Under the optimal condition ($P = 200$ nm, $F = 0.25$, $N = 32$, Au10nm-Si20nm); (b) for different filling factors (F) ($P = 200$ nm, $N = 32$, Au10nm-Si20nm); (c) for different total number of metal/dielectric pairs (N) ($P = 200$ nm, $F = 0.25$, Au10nm-Si20nm); (d) for different components in one pair ($P = 200$ nm, $F = 0.25$, $H = 960$ nm).

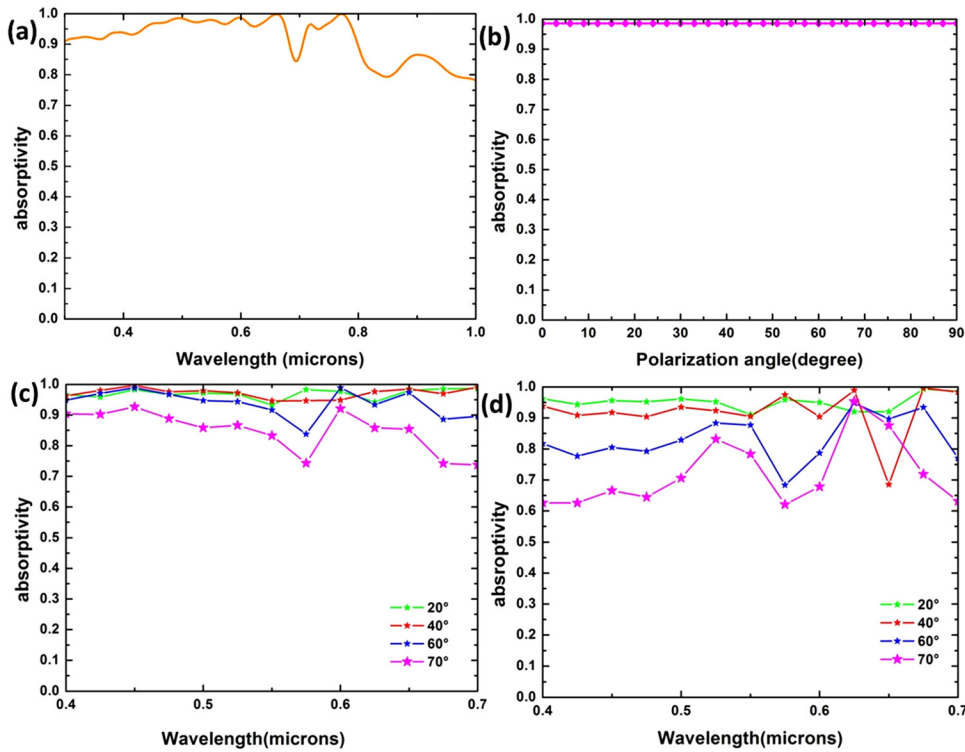


FIG. 3. Absorption spectra for meta-nanopillar absorber under various conditions. (a) The waveband of 300 nm–1000 nm; (b) different polarization states when incident wavelength is 600 nm under the normal incident angle; (c) different incident angles of 20°, 40°, 60°, and 70° for TM wave; (d) different incident angles of 20°, 40°, 60°, and 70° for TE wave.

explained by the local excitation of surface plasmon resonance induced by the incident light in the interface of metallic/dielectric.¹⁴ Since the surface plasmons only propagate along the metal/dielectric interface, electric field intensity is enhanced at the edges of the meta-nanopillar. As can be seen from Fig. 5, the enhancement effects are more pronounced for wavelengths of 506 nm and 613 nm with no

less than four hot spots on each edge of the nanopillar, which is consistent with the two absorption peaks shown in Fig. 2(a). While for wavelengths of 650 nm and 700 nm, it is obvious that the electric field intensity enhancement at the edges of meta-nanopillar is relatively weak. This means localized surface plasmon enhancement effect is relatively weak for these two wavelengths and the strong absorption at

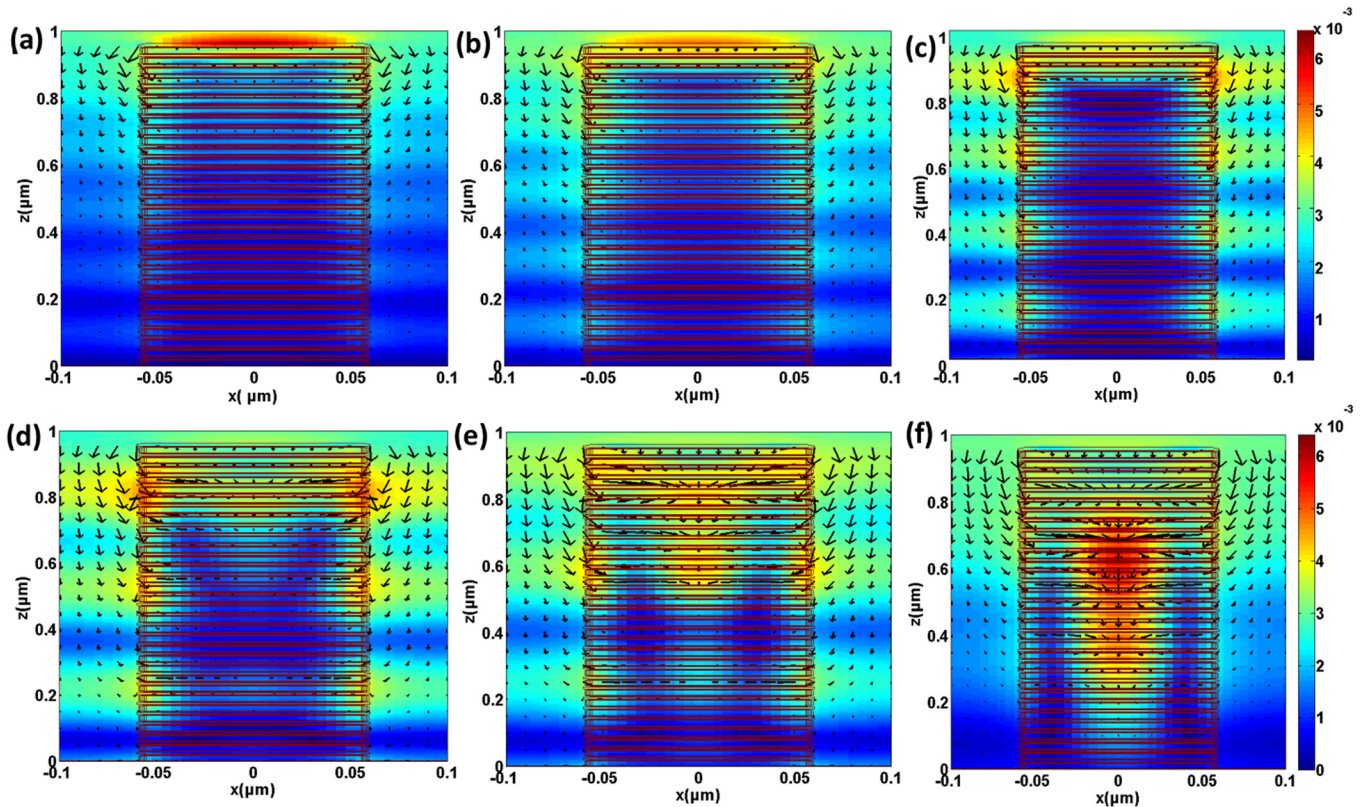


FIG. 4. Distribution of magnetic field $|H_y|$ and energy flow (black arrow) for the metamaterial nanopillar absorber at various wavelengths. (a) $\lambda = 400$ nm; (b) $\lambda = 450$ nm; (c) $\lambda = 506$ nm; (d) $\lambda = 613$ nm; (e) $\lambda = 650$ nm; (f) $\lambda = 700$ nm.

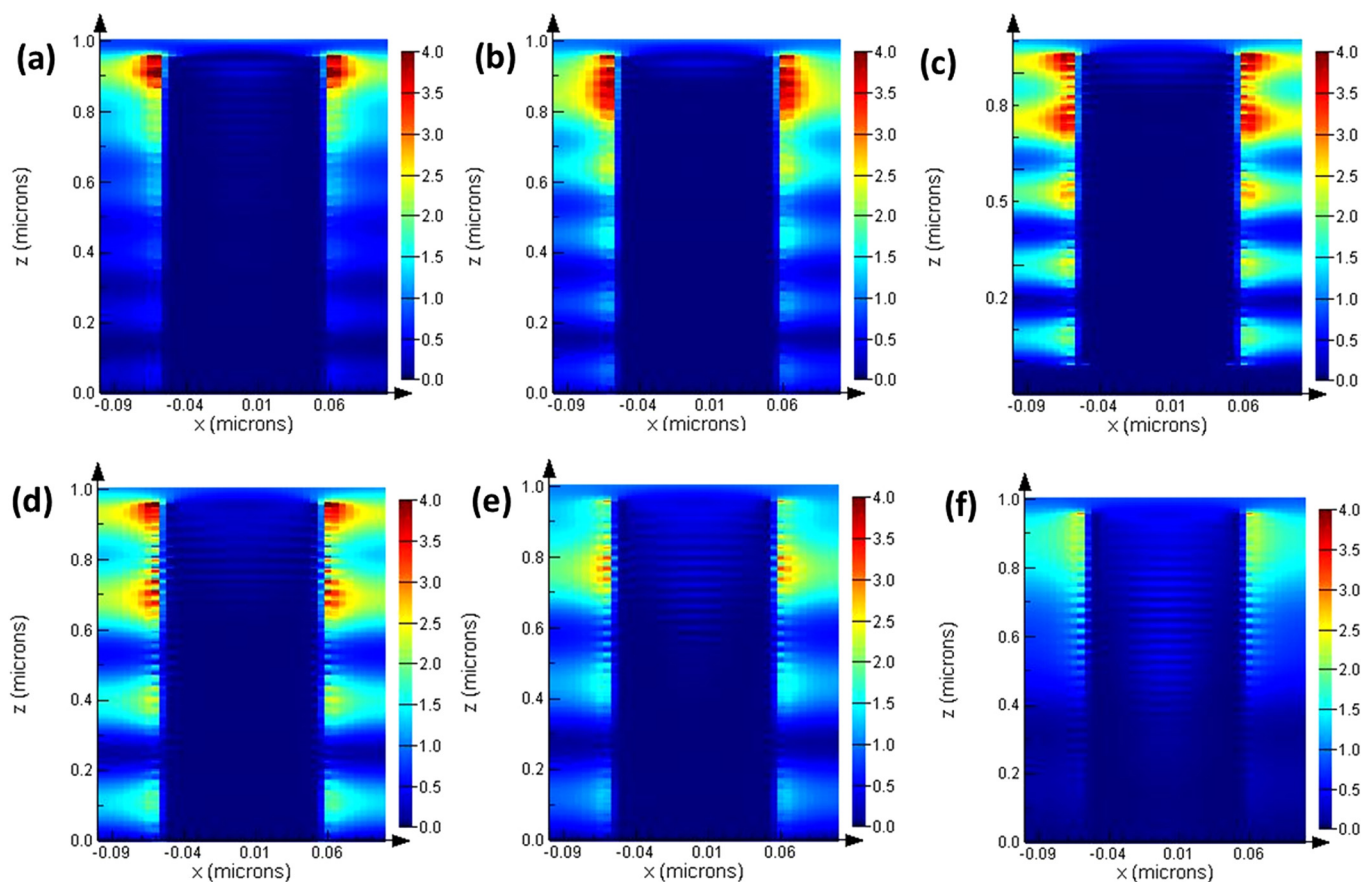


FIG. 5. Electric $|E_x|$ distribution at $y=0$ plane for different wavelengths. (a) $\lambda=400$ nm; (b) $\lambda=450$ nm; (c) $\lambda=506$ nm; (d) $\lambda=613$ nm; (e) $\lambda=650$ nm; (f) $\lambda=700$ nm.

these two wavelengths should be mainly attributed to slow light mode effect.

Therefore, by considering both results shown in Figs. 4 and 5 and discussions mentioned above, we can conclude that the physical mechanism for the strong absorption of sub-wavelength meta-nanopillar array is the synergistic effect of slow light mode and localized surface plasmon enhancement. The former effect is more pronouncing for longer wavelength while the latter effect is more pronouncing for shorter wavelength.

In conclusion, we have proposed a two-dimensional periodic meta-nanopillar array which can achieve an average absorptivity of 0.96 in the whole visible waveband. The absorber is shown to be insensitive to the light polarization state and able to retain very high absorptivity at a very large incident angle of $\pm 60^\circ$. This high absorptivity of meta-nanopillar array is explained as the synergistic effect of the slow light mode and the localized surface plasmon resonance enhancement. With the vast demand of the sustainable and green energy nowadays, we believe that the proposed absorber will find its application in those areas related with light harvesting.

The authors acknowledge the financial supports from the Ministry of Science and Technology of China under

Grant No. 2010DFR10660 and the Zhejiang Provincial Nature Science Foundation of China under Grant No. Y1111024.

- ¹L. He, C. Jiang, Rusli, D. Lai, and H. Wang, *Appl. Phys. Lett.* **99**, 021104 (2011).
- ²O. Muskens, J. Rivas, R. Algra, E. Bakkers, and A. Lagendijk, *Nano Lett.* **8**, 2638–2642 (2008).
- ³C. Lin and M. Povinelli, *Opt. Express* **17**, 19371–19381 (2009).
- ⁴H. Fang, X. Li, S. Song, Y. Xu, and J. Zhu, *Nanotechnology* **19**, 255703 (2008).
- ⁵M. Kelzenberg, D. Turner-Evans, B. Kayes, M. Filier, M. Putnam, N. Lewis, and H. Atwater, *Nano Lett.* **8**, 710–714 (2008).
- ⁶T. Stelzner, M. Pietsch, G. Andrä, F. Falk, E. Ose, and S. Christiansen, *Nanotechnology* **19**, 295203 (2008).
- ⁷L. Hu and G. Chen, *Nano Lett.* **7**, 3249–3252 (2007).
- ⁸J. Zhu, Z. Yu, G. Burkhard, C. Hsu, S. Connor, Y. Xu, Q. Wang, M. McGehee, S. Fan, and Y. Cui, *Nano Lett.* **9**, 279–282 (2009).
- ⁹J. Li, H. Yu, S. Wong, G. Zhang, X. Sun, P. Lo, and D. Kwong, *Appl. Phys. Lett.* **95**, 033102 (2009).
- ¹⁰Y. Huang, S. Chattopadhyay, Y. Jen, C. Peng, T. Liu, Y. Hsu, C. Pan, H. Lo, C. Hsu, Y. Chang, C. Lee, K. Chen, and L. Chen, *Nat. Nanotechnol.* **2**, 770–774 (2007).
- ¹¹S. Han and G. Chen, *Nano Lett.* **10**, 1012–1015 (2010).
- ¹²Y. Cui, J. Xu, K. Fung, Y. Jin, A. Kumar, S. He, and X. Fang, *Nano Lett.* **12**, 1443–1447 (2012).
- ¹³Q. Liang, T. Wang, Z. Lu, Q. Sun, Y. Fu, and W. Yu, *Adv. Opt. Mater.* **1**, 43–49 (2013).
- ¹⁴J. Hao, J. Wang, X. Liu, W. J. Padilla, L. Zhou, and M. Qiu, *Appl. Phys. Lett.* **96**, 251104 (2010).